J Electroceram (2007) 19:295–301
DOI 10.1007/s10832-007-9038-1

The investigation of key processing parameters in fabrication of $Pb(Zr_xTi_{1-x})O_3$ thick films for MEMS applications

S. Corkovic · Q. Zhang · R. W. Whatmore

Received: 21 March 2006 / Accepted: 19 October 2006 / Published online: 7 March 2007

Abstract It has always been a big challenge to deposit dense and crack-free $Pb(Zr_xTi_{1-x})O_3$ (PZT) thick films through Chemical Solution Deposition (CSD). In this study, a sol with higher concentration (≥0.6 M) was spun onto a platinised silicon substrate. The single layer thickness of a dense, crack-free film with several tenths of nanometres up to 350 nm could be obtained. It was found that the key factor in obtaining thick crack-free films was to choose an appropriate heating profile. In this study, the deflection of a single layer at various stages of heating was analysed through the measurement of the wafer curvature using the Dektak profilometer. As a result three characteristic changes of deflection were found, happening at 300, 450 and 500 °C. These obvious changes in wafer deflection closely relate to the transformations of sol-to-gel, gel-to-amorphous solid and amorphous solid-to-solid crystals. Furthermore, using these temperatures to thermally treat each single layer, it was possible to obtain thick crack-free films by repeatedly spin coating. The dielectric and piezoelectric properties, such as $d_{33,f}$ and $e_{31,f}$, of the films with different thicknesses and orientations were measured and compared.

Keywords PZT · Thick film · Sol-gel · Piezoelectrics · Stress · Orientation

1 Introduction

Interest in ferroelectric thin films has been considerable over the last 20 years and has been driven by the exciting possibility of using them for non-volatile memory applications [1] and new microelectromechanical systems (MEMS) [2–4]. Ferroelectric thin films can be prepared by a number of different deposition methods [5–12]. The sol-gel method is preferred for many applications because it offers both compositional control and reduced-temperature processing of highly uniform, dense, crack-free films. To exploit the advantageous PZT properties (such as high $d_{33,f}$ coefficient) in a wide range of piezoelectric actuator applications, thick films are needed, from several microns to several 10s of microns [13]. Although thick sol-gel films can be achieved by multiple layer coating techniques (thickness of each single layer <100 nm), repetitive layer coating is time consuming and impracticable in the industries. Many attempts were undertaken to increase the single layer thickness and so to reduce the quantity of the processing steps. When the thickness of a single layer increases, it simultaneously increases the internal stress due to the thermal mismatch between the PZT film and the substrate, which easily leads to the cracks of the films. Hence, the main challenge herein is to produce a crack free and dense thick film on the platinised silicon substrate. The single layer thickness can be increased easily by mixing a PZT powder and PZT sol to create a slurry [14] or by adding polymers [15]. Although latter films exhibit good piezoelectric properties, the residual pore contents and random orientation are limiting the performance of the films. The main aim of this study is to deposit thick PZT films through controlling key processing parameters, such as concentration and heating profile, in order to allow an increase of the crack-free single layer thickness while retaining the same piezoelectric properties as known for thin films.

S. Corkovic (✉) · Q. Zhang · R. W. Whatmore
Department of Advanced Materials,
Cranfield University,
Beds MK43 0AL, UK
e-mail: s.corkovic@cranfield.ac.uk

2 Experimental

$Pb(OOCCH_3)_2\ 3H_2O$ was dissolved in CH_3OH with heating. $Ti(O^nBu)_4$ and $Zr(O^nPr)_4$ Pr^nOH were mixed together and

dissolved in a mixed solution of CH_3COOH and CH_3OH. The molar ratio of Zr/Ti was equal to 40/60. Two solutions were then mixed together and refluxed for 2 h. Pb excess was fixed at 10 mol% to compensate for Pb loss during the heat treatment. The concentration of the solution was 0.6 M based on Pb content. A typical thickness of a single layer spun at 2,000 rpm is 200 nm. All heating experiments were conducted on a hotplate in an ambient air.

To find the processing temperatures the wet layers were exposed to temperatures in the range between 100 and 600 °C starting with low temperature and increasing the temperature gradually. At each temperature the film was heated for one minute, and then cooled down to room temperature. A wafer deflection measurement was taken using the Dektak surface profilometer and the film was heated for another minute at the same temperature followed by another wafer deflection measurement. This is referred to as one cycle at a temperature. After one such cycle the film was treated at the next higher temperature and the same cycle was performed.

The wafer deflection measurement was performed always along the same line across the wafer, using a self designed and constructed jig assuring the accuracy of the measurement. Thicker films were obtained by repeated deposition of thin layers on the substrate. The deflection measurement during the multilayer film deposition was performed after each treatment at characteristic temperature after the film was cooled down to room temperature. The orientation of each film was determined by the standard θ–2θ X-ray diffraction (XRD) method on a Siemens D5005 diffractometer using CuK_α radiation and a Goebel mirror. The peaks were deconvoluted and the integral intensities were determined for all detected peaks. The peak intensities were normalized according to [16] and compared with the powder diffraction files from the PCPDF database. Film cross-sections were prepared by fracture and examined using a SEM (Philips FSEM XL30). For the measurement of electrical properties, a set of Au/Cr electrode dots was evaporated onto the film surface through stainless steel shadow mask (diameter 2 mm). The exposed Pt bottom electrode beneath the film provided the counter-electrode. Film thickness was determined from a Dektak surface profilometer, and compared against values taken from the SEM cross-section images. The dielectric constant and loss tangent of the PZT films at frequency 1 kHz were measured using a WK Wayne Kerr Precision Component Analyser 6425. Piezoelectric measurements of $d_{33,f}$ and $e_{31,f}$ coefficients were performed using a Take Control Berlincourt Piezometer as described by [17]. The samples were poled at 200 °C with the field for 2 μm=125 kV/cm, 3 μm=83 kV/cm and 50 kV/cm for 5 μm thick film.

3 Results and discussion

3.1 Stress development in single PZT layer

Figure 1 shows the results of the wafer deflection measurement during the processing of a single layer. Positive and negative deflection values stand for convex and concave bending of the wafer, respectively. From the deflection results (Fig. 1) four stages or temperature ranges could be distinguished. They were between 100 and 300, 300 and 450, 450 and 500, and above 500 °C, respectively.

Before PZT deposition the maximum convex wafer deflection was around 10 μm due to sputtered platinum electrode. After PZT deposition of a single 200 nm thick layer and exposing it to high temperatures the deflection was found to decrease. The wafer shape was becoming flatter as the heating profile was approaching 300 °C. At 300 °C the wafer was flat. This can be interpreted as stress-free since very low deflection was measured. In this temperature range corresponding to the transformation from sol to gel, various reactions take place i.e., evaporation of the organic substance and water, resulting in the drying of the gel and polymerization, as reported by [18] and [19]. At this stage, the film experienced a major volume loss [20] resulting in shrinkage of the film [21] and thus decreased the strong compressive deflection. Above 300 °C the shape of the wafer changed to concave deflection due to the further shrinkage of the PZT film. In the temperature range between 300 and 450 °C the deflection increased linearly with the increase of temperature until 450 °C. In this temperature range the magnitude of the deflection increase is relatively small and it corresponds to the transformation of gel-to-amorphous solid. The deflection of the film thermally treated at between 450 and 500 °C started to

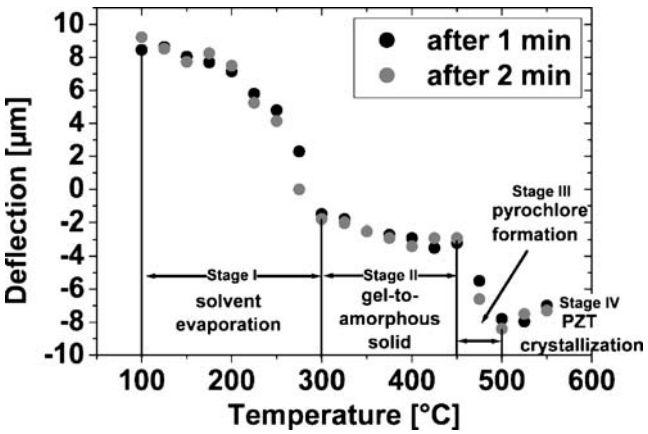

Fig. 1 Wafer deflection of 200 nm thick PZT 40/60 film on platinised substrate

increase rapidly. In this temperature range, the deflection increased for about 4 μm. Figure 2 shows XRD patterns of a PZT film thermally treated at different temperatures. For the film thermally treated at 450 °C, a peak appeared at around 2θ=29.8°, which indicates the formation of pyrochlore phase, and also implies that the pyrochlore formation is inducing large tensile stresses into the film as earlier observed by [22]. When the thermal treatment temperature was further increased to 500 °C and above, the deflection started to decrease and reached a final value of −7 μm. The corresponding XRD patterns of the film thermally treated at between 500 and 550 °C are shown in Fig. 3. PZT perovskite peaks are visible in the film heat-treated at 500 °C though some pyrochlore existed. When thermally treated above 550 °C, pyrochlore phase was completely transformed to perovskite. The tensile stress was partially relaxed during crystallisation of PZT. The stress relaxation can be either due to the crystallisation into paraelectric cubic phase itself or due to the phase transition at Curie temperature or a combination of both. However, lower tensile deflection after crystallization was observed.

The wafer deflection values after thermal treatment for 1 or 2 min at the same temperature were almost the same except at 275 and 475 °C. At the latter two temperatures the change of deflection is too large to be attributed to the measurement error. The fact that the deflection had nearly the same values after 1 and 2 min shows that all stress related processes are finished already after 1 min of thermal treatment. If the samples are treated at the same temperature for longer than 1 min, no significant change was found. At 275 and 475 °C the changes in the film were not as fast and the ongoing processes in the film needed longer time to complete. This results give some indication about the required minimum baking time for the PZT sol-gel films.

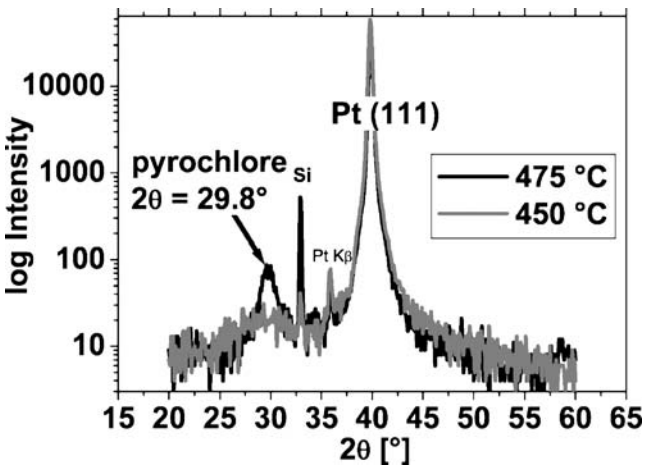

Fig. 2 XRD pattern of the sol-gel film after baking at 475 and 450 °C

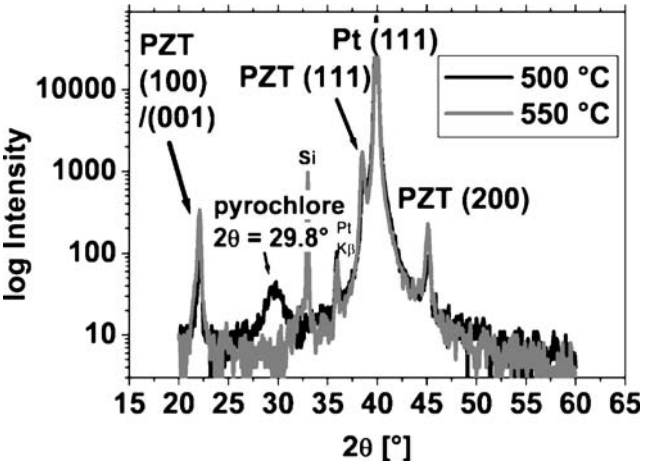

Fig. 3 XRD pattern of the sol-gel film after baking at 500 and 550 °C

3.2 Stress development in PZT multilayers

To build up a thick film, four thermal treatment temperatures based on the measurement of deflection in the single layer processing were used. They were 100, 300, 450 and 550 °C, corresponding to the starting points of four temperature ranges of deflection change. Each layer was treated at the same temperatures in sequence. The treatment duration is stated in the Fig. 4. The deflection was measured after the film was cooled down to room temperature in between each heating stage. The use of these thermal treatment temperatures made it possible to increase a crack-free single layer thickness. If e.g., other temperatures than indicated in Fig. 1 were used to process the PZT films it was found that the films would develop cracks after the deposition of only two or three layers (0.4–0.6 μm).

During the processing of the first PZT layer, a large deflection change was found. Wafer deflection changed from

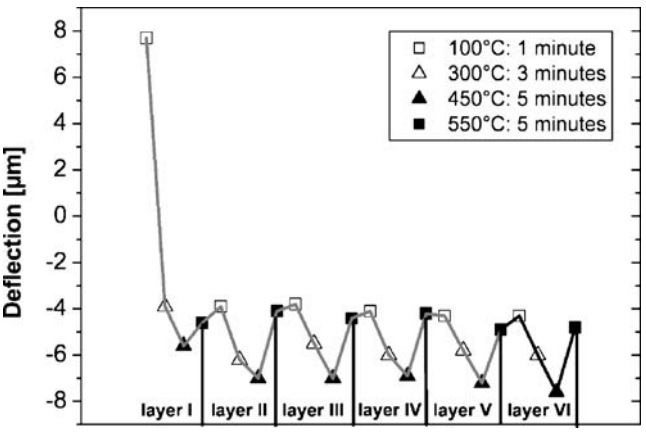

Fig. 4 Deflection during multilayer film coating

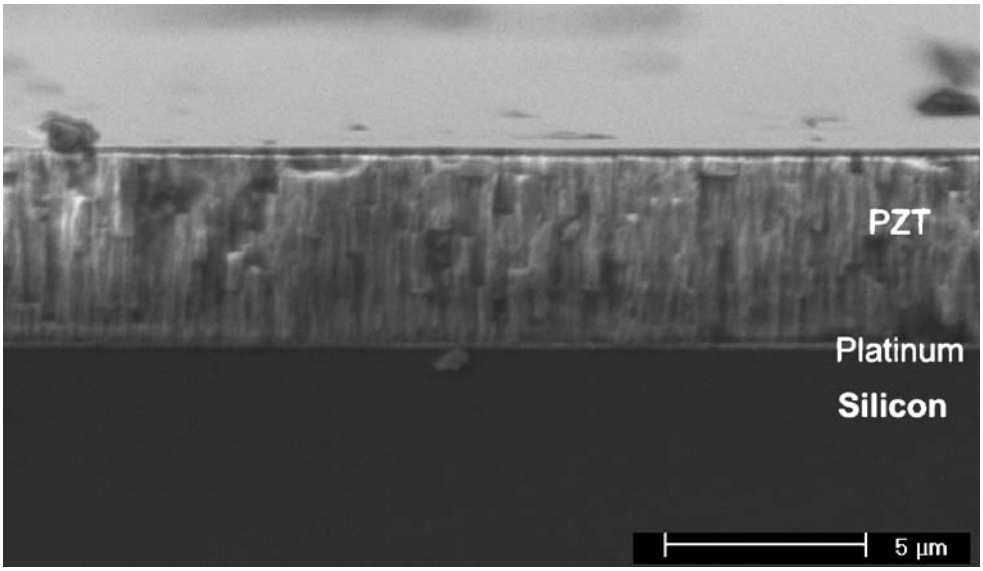

Fig. 5 Cross section (SEM) of 5 µm thick (25 layers) film fabricated using heating profile

8 to −4 µm in total. The major increase was found in the first processing stage after drying at 100 °C and baking at 300 °C. A further small deflection increase was found again at 450 °C due to pyrochlore formation. After the film crystallisation some relaxation was observed. From the deposition and processing of the second layer again the deflection increased at 300 and 450 °C whereas the film relaxed above 500 °C. Such cyclic behaviour of the deflection could be observed in the processing of each additional layer. The resultant deflection after film crystallisation gave rise to similar values ranging between −7 and −8 µm and indicating tensile stresses. If these temperatures were used to build up a thick film, the resulting residual stresses would not change significantly during the multilayer deposition. Figure 5 shows a SEM cross-section image of a PZT film with a thickness of 5 µm. The film was prepared by using these four thermal treatment temperatures described above for each layer. The thickness of each layer was 200 nm. The film was dense and crack-free.

3.3 Substrate influence on stresses in PZT films

Compressive stress was usually found to be in as-sputtered platinum layer, as reported by [23, 24]. The compressive stress can be released if the platinum layer was heated to the maximum processing temperature (550 °C here). Usually, tensile stress is found after cooling down to room temperature. During platinum annealing the defects in the microstructure related to the sputtering process can be healed and the stresses change from compressive to tensile. In Fig. 6 two AFM images of as-sputtered platinum and of the annealed platinum are depicted. A larger grain size could be observed in the annealed platinum. The film was annealed at 550 °C for 30 min. The sign of stress was purely the product of thermal expansion mismatch between platinum layer and silicon wafer. This process of defects healing and the stress relaxation in platinum could simultaneously happen during the PZT film processing [25]. Hence, the wafer deflection was not only the result of

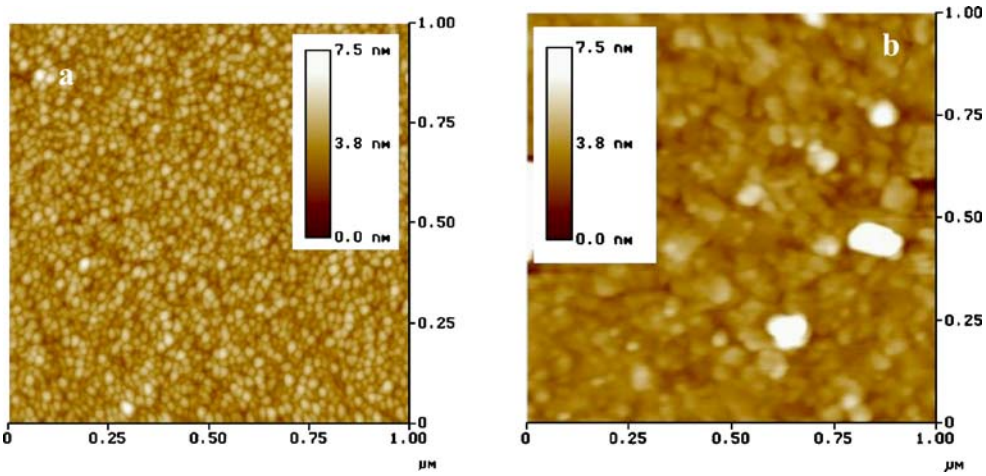

Fig. 6 AFM pictures of platinum grain size **a** as sputter deposited and **b** after annealing for 30 min at 550 °C

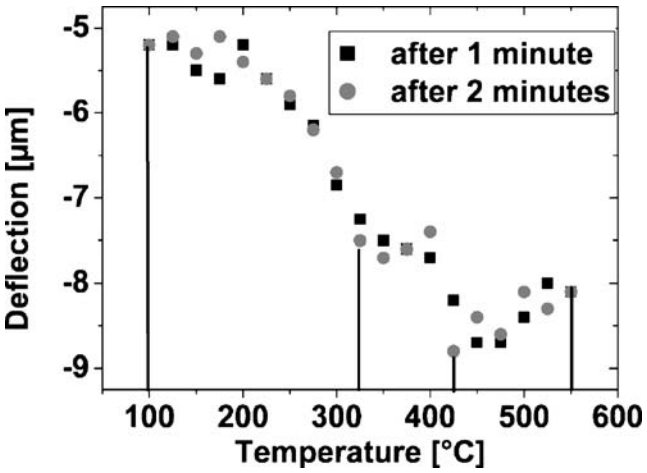

Fig. 7 Deflection measurement results during film processing on pre-annealed platinum substrate

intrinsic film stresses due to film shrinkage, and the extrinsic stresses due to the thermal expansion mismatch between the PZT film and the substrate layers, but also a result of the relaxation processes in the platinum bottom electrode. To exclude the contribution of platinum relaxation to the wafer deflection, a platinised Si wafer was annealed at 600 °C for 10 min prior to PZT deposition. The stress in platinum changed from compression to tension. A single PZT layer was then deposited on the pre-annealed platinum. The results of the deflection measurements are shown in Fig. 7.

The wafer deflection before PZT deposition was negative indicating tensile stresses. The deflection behaviour was very similar to that shown in Fig. 1. The four temperature ranges in Fig. 7 could be identified though the temperature ranges were slightly shifted. This small shift of the temperature ranges could have been caused by the experimental error. It is also possible that the nucleation behaviour of PZT on pre-annealed platinum differs slightly and enables lower pyrochlore formation and PZT crystallization temperature. In all temperature ranges in Fig. 7 lower total deflection change values were found, e.g., in the pyrochlore formation temperature range, the deflection increase in Fig. 1 was larger, around 4 µm, whereas it was only 1 to 1.5 µm in Fig. 7. This result indicates that although the substrate with pre-annealed Pt affected the wafer deflection, a significant contribution to the wafer deflection came from the PZT film. As shown in the Fig. 4 the platinum-related deflection change was completed after the first PZT layer was deposited and heat-treated. There was no further influence on the following PZT layers. Once the stress in platinum was released with the grain growth, the stress in platinum would not change during further PZT deposition. The wafer bending was induced solely by the incremental stresses in the PZT film layer.

During PZT film processing the ocurring stresses cause the wafer to bend. As shown in the Section 3.1 some major processes in the PZT film could be identified using the wafer deflection method together with X-ray diffraction. The thermal treatment of the PZT films from room temperature to high temperature is associated with the following changes in the film: evaporation of the solvent, burn-off of organic contents, pyrochlore formation and the transformation of pyrochlore to perovskite. Each of these changes induces a certain amount of stress. If the amount of simultaneously induced stress is very high, the films tend to crack. By choosing the above temperature profile, each individual process is being separated from the others. The first process in the film is allowed to finish before the next one can start. Thus the amount of stress induced at one time is limited and controlled. If the films are fired at other temperatures than indicated in Fig. 1, all processes in the film would simultaneously happen or would overlap, giving rise to high stresses. The film would crack easily.

This result suggests that for each different sol on a different type of substrate and different substrate materials the wafer deflections should be measured, as shown in Section 3.1, if ideal processing parameters are desired to produce a crack-free and dense film.

3.4 Piezoelectric and dielectric properties

Piezoelectric and dielectric coefficients for PZT 40/60 film with different thickness and orientation are summarised in Table 1. All films were treated at the same temperatures as shown in Fig. 1, but for different period of time. The

Table 1 Piezoelectric properties and orientation of PZT thick films.

Sample thickness	2 µm	3 µm thick films							5 µm
Orientations	(111)	(100)	(100)	(100)	(100)	(111)	mixed	(111)	(100)
$d_{33,f}$ [pC/N]	−59±1	−82±2	−82±2	−76±1	−82±1	−68±1	−82±1	−67±1	−160±30
$e_{31,f}$ [C/m^2]	7.17	10	9.8	9.22	9.86	7.89	8.46	8.86	9.02
$\varepsilon_{33,f}$	547±7	511±13	544±8	550±7	518±9	400±14	559±2	569±20	634±11
tan δ	0.018	0.016	0.015	0.013	0.016	0.014	0.016	0.017	0.017

The thickness of each layer was 200 nm.

different holding times at indicated temperatures resulted in different orientations. In the X-ray diffraction patterns no other peaks were detected than those resulting from the lattice plains (100)/(001), (110), (111) and (002)/(200), respectively, showing high degree of preferred orientation. Typical normalized intensity of (100)/(001) orientated films was higher than 0.9 whereas it was slightly lower for (111) orientated films, around 0.7.

The maximum single layer thickness that could be obtained with this sol concentration was 350 nm at spin speed 1,000 rpm. One such film is included, underlined in the Table 1. Due to the low spin speed the film surface exhibited some surface roughness and it was decided to carry out the work only on films with 200 nm of single layer thickness. Hence, all other films had single layer thickness of 200 nm.

The measurement results in Table 1 show higher piezoelectric coefficients with the increase of film thickness. The $d_{33,\,f}$ coefficient was found to be sensitive to film thickness and was higher in thicker films. Also, some influence of the crystalline orientation on the $d_{33,f}$ was found, showing higher values for (100)/(001) oriented films. The coefficient $e_{31,f}$ was also higher in films with (100)/(001) orientation and shows no dependency on film thickness. Similar results for PZT 40/60 were reported by [26]. The 5 μm thick film showed higher $d_{33,f}$ than the bulk material, reported in [27]. The reason for higher $d_{33,f}$ values in thicker films is probably the higher degree of (100)/(001) orientation in such films. Close to the platinum substrate the PZT films tend to have (111) preferred orientation due to the lattice match between Pt(111) and PZT(111). However, the lattice plain (100) is the plain with fastest growth kinetics. As more layers are deposited the growth in <100> direction will out rule the growth in <111> direction and as a result a high (100) orientation and only few (111) crystallites in thick films are obtained. As it can be observed on films with equal thickness, higher coefficients were found in (100) oriented films. Hence, the reason for higher $d_{33,f}$ in 5 μm thick film than in bulk can be found in the high degree of orientation. The $d_{33,f}$ value in this film is close to the maximum value for tetragonal PZT films proposed by [28], probably lower if high spread is considered.

The reason why $e_{31,f}$ coefficient is not thickness dependent could be sought in the stress state of the films. According to the deflection measurement from Fig. 4 the stress increase with thickness increase is very low. Thus it can be assumed that for all thicknesses nearly the same stress state can be found.

Dielectric constant for all films was in the range between 500 and 600. Due to small number of (111) oriented samples and the measurement spread no influence of the orientation on the dielectric properties could be found. The dielectric loss is below 0.02 for most of the films.

4 Conclusions

Thicker PZT films were obtained by increasing the sol concentration. The stress development during the processing of PZT films has been analysed by measuring the wafer deflection. The influence of substrate on the stress development of PZT films was also analysed. The key processing parameters can be obtained through measuring the wafer bending. Using these key temperatures to treat each layer, thicker crack-free single layers of PZT can be obtained. The maximum single layer thickness was 350 nm by using the described sol concentration. The thick films deposited using thick single layers exhibit good piezoelectric coefficients in comparison with the films obtained with thinner single layers. As an example, a 5 μm thick PZT film was prepared with 25 layers. The $d_{33,f}$ value (160 pC/N) of this film is higher than of its corresponding bulk material and close to the maximum expected value for tetragonal thin film.

Acknowledgement The financial support of EPSRC through project GR/S45027/01 is gratefully acknowledged. The Authors would like to thank Miss C. Kimpton for the AFM images.

References

1. J.F. Scott, C.A. Paz de Arajuo, Science **246**, 1400 (1989)
2. P. Muralt, IEEE Trans. Ultrason. Ferroelectr. Freq. Control **47**, 903 (2000)
3. P. Muralt, J. Micromechanics Microengineering **10**, 136 (2000)
4. A.M. Flynn, L.S. Tavsrow, S.F. Bart, R.A. Brooks, D.J. Ehrlich, K. Udayakumar, L.E. Cross, J. Microelectromech. Syst. **1**, 44 (1992)
5. R.N. Castellano, L.G. Feinstein, J. Appl. Phys. **50**, 4406 (1979)
6. S.B. Krupanidhi, N. Maffeo, M. Sayer, K. El-Asselet, J. Appl. Phys. **54**, 6601 (1983)
7. K. Sreenivas, M. Sayer, P. Garrett, Thin Solid Films **172**, 251 (1989)
8. S. Otsubo, T. Maeda, T. Minamikawa, Y. Yonezawa, A. Morimoto, T. Shimizu, Jpn. J. Appl. Phys. **29**, L133 (1990)
9. B.S. Kwak, E.P. Boyd, A. Erbil, Appl. Phys. Lett. **53**, 1702 (1988)
10. K. Sreenivas, M. Sayer, D.J. Baar, M. Nishioka, J. Appl. Phys. **54**, 6601 (1988)
11. K.D. Budd, S.K. Dey, D.A. Payne, Br. Ceram. Proc. **36**, 107 (1985)
12. S.K. Dey, K.D. Budd, D.A. Payne, IEEE Trans. UFFC **35**, 80 (1988)
13. R.W. Whatmore, Q. Zhang, Z. Huang, R.A. Dorey, Mater. Sci. in Semicond. Process. **5**, 65–76 (2003)
14. R.A. Dorey, R.D. Haigh, S.B. Stringfellow, R.W. Whatmore, Br. Ceram. Trans. **101**, 4 (2002)
15. H. Kozuka, S. Takenaka, H. Tokita, M. Okubayashi, J. Eur. Ceram. Soc. **24**, 1585–1588 (2004)
16. Harris, GB Phil. Mag. **43**, 113 (1952)
17. J.E.A. Southin, S.A. Wilson, D. Schmitt, R.W. Whatmore, J. Phys. D: Appl. Phys. **34**, 1456–1460 (2001)

18. C.D.E. Lakeman, Z. Xu, D.A. Payne, Proc. 9th ISAF IEEE Symp. 404–407 (1995)
19. G. Yi, Z. Wu, M. Sayer, J. Appl. Phys. **64**, 5 (1988)
20. C.D.E Lakeman, J.-F. Campion, D.A Suchicital, in *1990 IEEE 7th Int. Symp. on Appl. of Ferroelectrics* (Cat. No. 90CH2800-1, 1991), p. 681–4
21. G. Yi, M. Sayer, in *ISAF '92. Proc. of the Eighth IEEE Int. Symp. on Appl. of Ferroelectrics* (Cat. No.92CH3080-9, 1992) p. 289–92
22. B.A. Tuttle, J.A. Voigt, T.J. Garino, D.C. Goodnow, R.W. Schwartz, D.L. Lamppa, T.J. Headley, M.O. Eatough, in *Proceedings of the Eighth IEEE Int. Symp. on Appl. of Ferroelectrics*, (New York, 1992) pp. 344–348
23. E. Defay, C. Malhaire, C. Dubois, D. Barbier, Mater. Res. Soc. Symp. Proc. **594**, (2000)
24. L. Zhang, M. Ichiki, R. Maeda, J. Eur. Ceram. Soc. **24**, 1673–1676 (2004)
25. G.A.C.M. Spierings, G.J.M. Dormans, W.G.J. Moors, M.J.E. Ulenaers, P.K. Larsen, J. Appl. Phys. **78**, 1926 (1995)
26. N. Ledermann, P. Muralt, J. Baborowski, S. Gentil, K. Mukati, M. Cantoni, A. Seifert, N. Setter, Sens. Actuators A **105**, 162–170 (2003)
27. A. Garg, T.C. Goel, Mater. Sci. Eng. **B60**, 128–132 (1999)
28. X.-H. Du, U. Belegundu, K. Uchino, Jpn. J. Appl. Phys. **36**, 5580–5587 (1997)